Textile Dye Biodecolorization by MnP

Subjects: Biochemistry & Molecular Biology

Contributor: Tao Wang

Manganese peroxidase (MnP) is an oxidoreductase with ligninolytic activity and is a promising biocatalyst for the biodegradation of hazardous environmental contaminants, and especially for dye wastewater decolorization.

manganese peroxidase | biodecolorization | dye wastewater | immobilization | recombinant enzyme

1. Introduction

The textile industry produces large quantities of wastewater containing different types of dyes used during the dyeing process, which cause great harm to the environment [1][2]. Many dyes and their intermediate metabolites have been identified as mutagenic, teratogenic, or carcinogenic, and represent serious health threats to living ecosystems [3].

At present, the treatment of dye wastewater mainly relies on physical or chemical management techniques, including chemical reduction, adsorption, ionizing radiation, precipitation, flocculation and flotation, membrane filtration, electric coagulation, electrochemical destruction, and ion exchange ozonation [4][5]. These technologies have obvious shortcomings such as the excessive use of chemicals, sludge production, expensive factory requirements or high operating expenses, low decolorization efficiencies, and the inability to handle large numbers of dyes with different structures, so they are not economically suitable for large-scale wastewater decolorization [6].

The current focus is to reduce toxicity and develop an efficient, economical, and green dye detoxification and decolorization technology. Compared with physical and chemical methods, biological methods offer beneficial and effective prospects due to their economical and environmentally friendly advantages, as well as being simple to use, safe, and efficient, with no secondary pollution [7][8]. Therefore, biotechnology is considered the best choice to degrade and remove these pollutants effectively. In the biotechnology field, enzyme biocatalysis is currently the main research area due to its broad application prospects [9][10].

Manganese peroxidases (EC 1.11.1.13; MnPs) are a family of heme-containing glycoproteins belonging to the oxidoreductase group. It was discovered in *Phanerochaete chrysosporium* and is also found in many bacteria and white-rot fungi (WRF) [11][12][13][14]. There are different MnPs in nature with differentiated properties. For example, long and short MnPs were reported in WRF associated with the presence/absence of the C-terminal tail extension, and these showed different catalytic and stability properties [15]. According to the residues of the Mn^{2+}-binding site, three novel subfamilies of MnP were described in Agaricales including MnP-ESD (Glu/Ser/Asp Mn^{2+}-oxidation site),

MnP-DGD (Asp/Gly/Asp Mn^{2+}-oxidation site), and MnP-DED (Asp/Glu/Asp Mn^{2+}-oxidation site) [16]. However, the Mn^{2+}-binding site is not the unique feature of MnPs, because versatile peroxidases (VPs), which evolved directly from MnPs, also possess such a site and can oxidize Mn^{2+} to Mn^{3+} [17].

For enzyme applications, MnPs can catalyze the peroxide-dependent degradation of a variety of toxic dye pollutants, phenolic compounds, antibiotics, and polycyclic aromatic hydrocarbons, so are promising biocatalysts for hazardous environmental contaminants biodegradation [18][19]. Moreover, the use of MnPs is suitable for dye wastewater decolorization as the process is simple and the enzyme can be recycled, thus reducing operating costs [20][21][22].

2. The Crystal Structure of MnPs

The crystal structure of an enzyme provides information on the catalytic mechanism and for potential in-depth design and transformation, and for realizing the green biotechnological use of enzymes [23][24][25].

The heme conformation of MnP is similar to that of lignin peroxidase (LiP) and is evolutionarily conserved [26]. In its resting-state form, MnP is a strongly helical protein containing a Fe^{3+} penta-coordinated structure with the porphyrin ring of the heme cofactor and a proximal histidine, with the sixth coordination position open for H_2O_2 [27].

To date, several crystal structures of MnP from different sources have been reported, and the highest-resolution crystal structures (~0.93Å) of MnP complexed with Mn^{2+} (Mn-MnP) are shown in **Figure 1** [28]. The conserved Ca^{2+} ions are important for the stability of the protein [29]; these are indicated as gold yellow spheres and the position of the Mn^{2+} substrate is shown in violet. The active site is composed of three highly conserved amino acids (Glu35, Glu39, and Asp179) and one heme propionate. The Mn^{2+} substrate binds in the center of the active site, and the heme propionate (HEM) is located in the internal hydrophobic cavity of the enzyme. The spatial structure of HEM is further stabilized by four hydrogen bonds (green dashed line), two electrostatic interactions (orange dashed line), and some other weak interactions. The catalytic site of heme peroxidases is strongly conserved, with only minor variations occurring in the replacement of Phe with Trp in several enzymes such as ascorbate peroxidase and cytochrome c. The Asp–His pair (242 and 173, respectively) is also conserved.

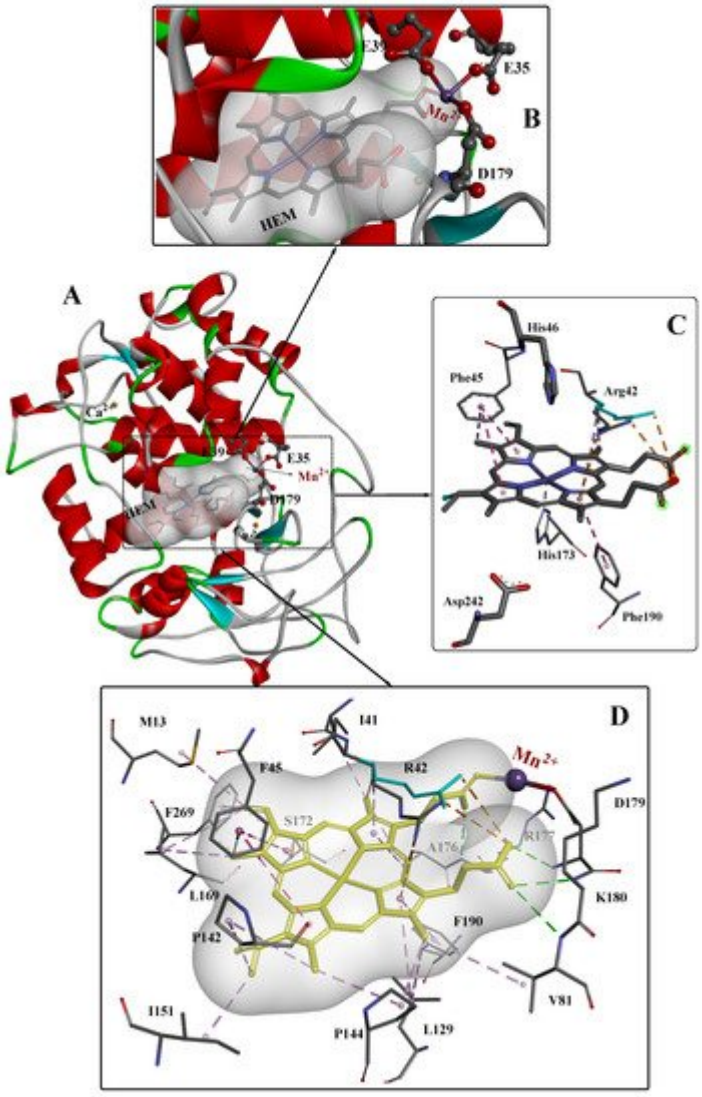

Figure 1. The overall structure (**A**), active site structure (**B**,**C**), and interaction mode (**D**) of Mn–MnP refined at 0.93 Å resolution [28]. PDB ID: 3M5Q.

3. MnP Catalysis

At the beginning of the catalytic cycle, H_2O_2 or organic peroxide binds to the enzyme in resting state in ferric (Fe^{3+}) form (**Figure 2**). This process releases one molecule of H_2O and forms MnP–compound I (Fe^{4+}-oxo-porphyrin radical complex), with two oxidation equivalents. This oxidizes Mn^{2+} to Mn^{3+}, forming MnP–compound II (Fe^{4+}-oxo-porphyrin complex). Immediately afterwards, the MnP–compound II combines with Mn^{2+} in a similar manner to generate Mn^{3+}, releasing one molecule of H_2O, and is reduced to the original state of ferric MnP, completing the catalytic cycle [30].

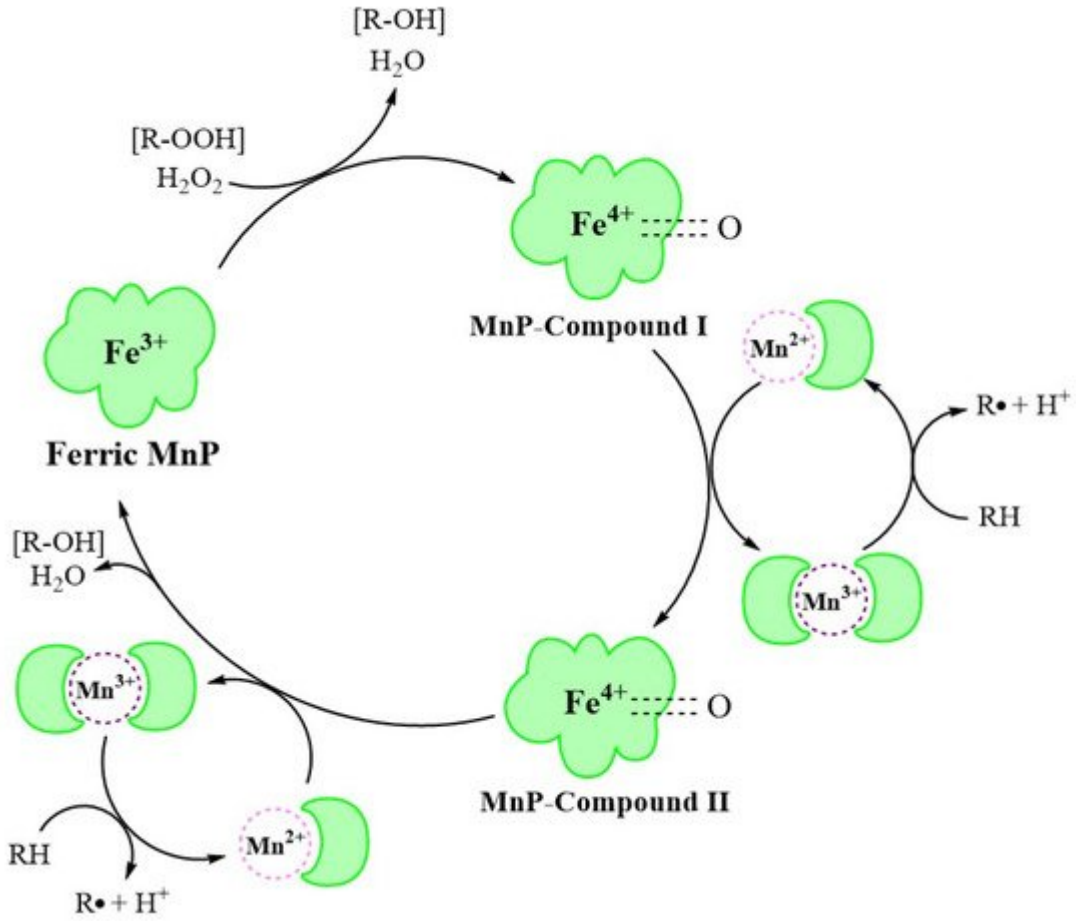

Figure 2. The MnP catalytic cycle [30].

The MnP catalytic cycle resembles that of other lignin and heme peroxidases in the presence of native Fe^{3+} enzymes and two reactive intermediates [31]. However, in contrast to other peroxidases, MnP preferentially uses Mn^{2+} as the substrate, converting it to the strong oxidation state of Mn^{3+} through a series of redox reactions [32].

4. Application of Unmodified MnPs in the Decolorization of Dye Wastewater

Table 1 contains a summary of recent studies on the breakdown and decolorization of textile-derived dye compounds by microbial MnPs.

Table 1. Recent applications of unmodified MnPs in dye decolorization.

Source	Types of Dyes	Initial Concentration of Dyes	Removal Rate	Time Cost	Reference
Microbial consortium SR	Crystal Violet	20 mg/L	63%	6 days	[20]

Source	Types of Dyes	Initial Concentration of Dyes	Removal Rate	Time Cost	Reference
	Cresol Red	100 mg/L	93%		
	CBB G250	100 mg/L	96%		
Trametes pubescens strain i8	Acid Blue 158	50 μM	95%	24 h	[22]
	Poly R-478		88%		
	Remazol Brilliant Violet 5R		76%		
	Direct Red 5B		66%		
	Indigo Carmine		64%		
	Methyl Green		50%		
	Cibacet Brilliant Blue BG		46%		
	Remazol Brilliant Blue Reactif		42%		
Aspergillus terreus GS28	Direct Blue-1	100 mg/L	98.4%	168 h	[33]
Bjerkandera adusta strain CX-9	Acid Blue 158	50 μM	91%	12 h	[34]
	Poly R-478		80%		

Source	Types of Dyes	Initial Concentration of Dyes	Removal Rate	Time Cost	Reference
	Cibacet Brilliant Blue BG		77%		
	Remazol Brilliant Violet 5R		70%		
	Indigo Carmine		94.6%		
Trametes sp.48424	Remazol Brilliant Blue R	100 mg/L	85.0%	18 h	[35]
	Remazol Brilliant Violet 5R		88.4%		
	Methyl Green		93.1%		
Microbial consortium ZSY	Metanil Yellow G	100 mg/L	93.39%	48 h	[36]
Microbial Consortium ZW1	Methanil Yellow G	100 mg/L	93.3%	16 h	[37]
Trichoderma harzianum	Alizarin Blue Black B	0.03%	92.34%	14 days	[38]
	Congo Red		41.84%		
Phanerochaete chrysosporium CDBB 686	Poly R-478	50 ppm	56.86%	36 h	[39]
	Methyl Green		69.79%		

Source	Types of Dyes	Initial Concentration of Dyes	Removal Rate	Time Cost	Reference
Bjerkandera adusta CCBAS 930	Alizarin Blue Black B	0.01%	86.5%	20 days	[40]
	Acid Blue 129		89.22%		
Cerrena unicolor BBP6	Congo Red	100 mg/L	53.9%	12 h	[41]
	Methyl Orange		77.6%	12 h	
	Remazol Brilliant Blue R		81.0%	5 h	
	Bromophenol Blue		62.2%	12 h	
	Crystal Violet		80.9%	12 h	
	Azure Blue		63.1%	24 h	
Phanerochaete chrysosporium	Indigo Carmine	30 mg/L	90.18%	6 h	[42]
Trametes versicolor	Dye mixture (Brilliant Blue FCF and Allura Red AC)	100 mg/L	80.45%	14 days	[43]
Irpex lacteus			86.04%	19 days	
Bjerkandera adusta			82.83%	9 days	

Source	Types of Dyes	Initial Concentration of Dyes	Removal Rate	Time Cost	Reference
Ceriporia lacerata ZJSY	Congo Red	100 mg/L	90%	48 h	[44]
Bacillus cohnni RKS9	Congo Red	100 mg/L	99%	12 h	[45]
Schizophyllum commune IBL-06	Solar Brilliant Red 80	0.01%	100%	3 days	[46]
Irpex lacteus CD2	Remazol Brilliant Violet 5R	50 mg/L	92.8%	5 h	[47]
	Remazol Brilliant Blue R		87.1%	5 h	
	Indigo Carmine		91.5%	5 h	
	Direct Red 5B		82.4%	36 h	

7. Ghosh, A.; Dastidar, M.G.; Sreekrishnan, T. Bioremediation of chromium complex dyes and treatment of sludge generated during the process. Int. Biodeterior. Biodegrad. 2017, 119, 448–460.
8. Kishor, R.; Saratale, G.D.; Saratale, R.G.; Ferreira, L.F.R.; Bilal, M.; Iqbal, H.M.; Bharagava, R.N. Efficient degradation and detoxification of methylene blue dye by a newly isolated ligninolytic enzyme producing bacterium Bacillus Albus MW407057. Colloids Surf. B Biointerfaces 2021, 206, 111947.
9. Gurung, N.; Ray, S.; Bose, S.; Rai, V. A Broader View: Microbial Enzymes and Their Relevance in Industries, Medicine, and Beyond. BioMed Res. Int. 2013, 2013, 329121.
10. Vilar, D.D.S.; Bilal, M.; Bharagava, R.N.; Kumar, A.; Nadda, A.K.; Salazar-Banda, G.R.; Eguiluz, K.I.B.; Ferreira, L.F.R. Lignin-modifying enzymes: A green and environmental responsive technology for organic compound degradation. J. Chem. Technol. Biotechnol. 2021, 96, 6751.
11. Kuwahara, M.; Glenn, J.K.; Morgan, M.A.; Gold, M.H. Separation and characterization of two extracelluar H2O2-dependent oxidases from ligninolytic cultures of Phanerochaete chrysosporium. FEBS Lett. 1984, 169, 247–250.

12. Glenn, J.K.; Gold, M.H. Purification and characterization of an extracellular Mn(II)-dependent peroxidase from the lignin-degrading basidiomycete, Phanerochaete chrysosporium. Arch. Biochem. Biophys. 1985, 242, 329–341.
13. Paszczyński, A.; Huynh, V.B.; Crawford, R. Enzymatic activities of an extracellular, manganese-dependent peroxidase from Phanerochaete chrysosporium. FEMS Microbiol. Lett. 1985, 29, 37–41.
14. Paszczyński, A.; Huynh, V.B.; Crawford, R. Comparison of ligninase-I and peroxidase-M2 from the white-rot fungus Phanerochaete chrysosporium. Arch. Biochem. Biophys. 1986, 244, 750–765.
15. Fernández-Fueyo, E.; Acebes, S.; Ruiz-Dueñas, F.J.; Martínez, M.J.; Romero, A.; Medrano, F.J.; Guallar, V.; Martínez, A.T. Structural implications of the C-terminal tail in the catalytic and stability properties of manganese peroxidases from ligninolytic fungi. Acta Crystallogr. Sect. D Biol. Crystallogr. 2014, 70, 3253–3265.
16. Ruiz-Dueñas, F.J.; Barrasa, J.M.; Sánchez-García, M.; Camarero, S.; Miyauchi, S.; Serrano, A.; Linde, D.; Babiker, R.; Drula, E.; Ayuso-Fernández, I.; et al. Genomic analysis enlightens Agaricales lifestyle evolution and increasing peroxidase diversity. Mol. Biol. Evol. 2021, 38, 1428–1446.
17. Ayuso-Fernández, I.; Ruiz-Dueñas, F.J.; Martínez, A.T. Evolutionary convergence in lignin-degrading enzymes. Proc. Natl. Acad. Sci. USA 2018, 115, 6428–6433.
18. Singh, A.K.; Bilal, M.; Iqbal, H.M.; Meyer, A.S.; Raj, A. Bioremediation of lignin derivatives and phenolics in wastewater with lignin modifying enzymes: Status, opportunities and challenges. Sci. Total. Environ. 2021, 777, 145988.
19. Bilal, M.; Bagheri, A.R.; Vilar, D.S.; Aramesh, N.; Eguiluz, K.I.B.; Ferreira, L.F.R.; Ashraf, S.S.; Iqbal, H.M. Oxidoreductases as a versatile biocatalytic tool to tackle pollutants for clean environment—A review. J. Chem. Technol. Biotechnol. 2021, 96, 1–44.
20. Yang, X.; Wang, J.; Zhao, X.; Wang, Q.; Xue, R. Increasing manganese peroxidase production and biodecolorization of triphenylmethane dyes by novel fungal consortium. Bioresour. Technol. 2011, 102, 10535–10541.
21. Bilal, M.; Asgher, M. Sandal reactive dyes decolorization and cytotoxicity reduction using manganese peroxidase immobilized onto polyvinyl alcohol-alginate beads. Chem. Cent. J. 2015, 9, 1–14.
22. Rekik, H.; Jaouadi, N.Z.; Bouacem, K.; Zenati, B.; Kourdali, S.; Badis, A.; Annane, R.; Bouanane-Darenfed, A.; Bejar, S.; Jaouadi, B. Physical and enzymatic properties of a new manganese peroxidase from the white-rot fungus Trametes pubescens strain i8 for lignin biodegradation and textile-dyes biodecolorization. Int. J. Biol. Macromol. 2019, 125, 514–525.

23. Engel, M.; Hoffmann, T.; Wagner, L.; Wermann, M.; Heiser, U.; Kiefersauer, R.; Huber, R.; Bode, W.; Demuth, H.-U.; Brandstetter, H. The crystal structure of dipeptidyl peptidase IV (CD26) reveals its functional regulation and enzymatic mechanism. Proc. Natl. Acad. Sci. USA 2003, 100, 5063–5068.
24. Qiu, J.; Wilkens, C.; Barrett, K.; Meyer, A.S. Microbial enzymes catalyzing keratin degradation: Classification, structure, function. Biotechnol. Adv. 2020, 44, 107607.
25. Chang, M.; Zhou, Y.; Wang, H.; Liu, Z.; Zhang, Y.; Feng, Y. Crystal structure of the multifunctional SAM-dependent enzyme LepI provides insights into its catalytic mechanism. Biochem. Biophys. Res. Commun. 2019, 515, 255–260.
26. Ayuso-Fernández, I.; Martínez, A.T.; Ruiz-Dueñas, F.J. Experimental recreation of the evolution of lignin-degrading enzymes from the Jurassic to date. Biotechnol. Biofuels 2017, 10, 1–13.
27. Blodig, W.; Smith, A.; Doyle, W.A.; Piontek, K. Crystal structures of pristine and oxidatively processed lignin peroxidase expressed in Escherichia coli and of the W171F variant that eliminates the redox active tryptophan 171. Implications for the reaction mechanism. J. Mol. Biol. 2001, 305, 851–861.
28. Sundaramoorthy, M.; Gold, M.H.; Poulos, T.L. Ultrahigh (0.93A) resolution structure of manganese peroxidase from Phanerochaete chrysosporium: Implications for the catalytic mechanism. J. Inorg. Biochem. 2010, 104, 683–690.
29. George, S.J.; Kvaratskhelia, M.; Dilworth, M.J.; Thorneley, R.N.F. Reversible alkaline inactivation of lignin peroxidase involves the release of both the distal and proximal site calcium ions and bishistidine co-ordination of the haem. Biochem. J. 1999, 344, 237–244.
30. Hofrichter, M. Review: Lignin conversion by manganese peroxidase (MnP). Enzym. Microb. Technol. 2002, 30, 454–466.
31. Wariishi, H.; Huang, J.; Dunford, H.; Gold, M. Reactions of lignin peroxidase compounds I and II with veratryl alcohol. Transient-state kinetic characterization. J. Biol. Chem. 1991, 266, 20694.
32. Wariishi, H.; Valli, K.; Gold, M.H.; Wariishi, H.; Valli, K.; Gold, M.H. Manganese(II) oxidation by manganese peroxidase from the basidiomycete Phanerochaete chrysosporium. Kinetic mechanism and role of chelators. J. Biol. Chem. 1992, 267, 23688–23695.
33. Singh, G.; Dwivedi, S. Decolorization and degradation of Direct Blue-1 (Azo dye) by newly isolated fungus Aspergillus terreus GS28, from sludge of carpet industry. Environ. Technol. Innov. 2020, 18, 100751.
34. Bouacem, K.; Rekik, H.; Jaouadi, N.Z.; Zenati, B.; Kourdali, S.; El Hattab, M.; Badis, A.; Annane, R.; Bejar, S.; Hacene, H.; et al. Purification and characterization of two novel peroxidases from the dye-decolorizing fungus Bjerkandera adusta strain CX-9. Int. J. Biol. Macromol. 2018, 106, 636–646.

35. Zhang, H.; Zhang, S.; He, F.; Qin, X.; Zhang, X.; Yang, Y. Characterization of a manganese peroxidase from white-rot fungus Trametes sp.48424 with strong ability of degrading different types of dyes and polycyclic aromatic hydrocarbons. J. Hazard. Mater. 2016, 320, 265–277.
36. Guo, G.; Hao, J.; Tian, F.; Liu, C.; Ding, K.; Zhang, C.; Yang, F.; Xu, J. Decolorization of Metanil Yellow G by a halophilic alkalithermophilic bacterial consortium. Bioresour. Technol. 2020, 316, 123923.
37. Guo, G.; Hao, J.; Tian, F.; Liu, C.; Ding, K.; Xu, J.; Zhou, W.; Guan, Z. Decolorization and detoxification of azo dye by halo-alkaliphilic bacterial consortium: Systematic investigations of performance, pathway and metagenome. Ecotoxicol. Environ. Saf. 2020, 204, 111073.
38. Rybczyńska-Tkaczyk, K.; Święciło, A.; Szychowski, K.; Kornitłowicz-Kowalska, T. Comparative study of eco- and cytotoxicity during biotransformation of anthraquinone dye Alizarin Blue Black B in optimized cultures of microscopic fungi. Ecotoxicol. Environ. Saf. 2018, 147, 776–787.
39. Sosa-Martínez, J.D.; Balagurusamy, N.; Montañez, J.; Peralta, R.A.; Moreira, R.D.F.P.M.; Bracht, A.; Peralta, R.M.; Morales-Oyervides, L. Synthetic dyes biodegradation by fungal ligninolytic enzymes: Process optimization, metabolites evaluation and toxicity assessment. J. Hazard. Mater. 2020, 400, 123254.
40. Rybczyńska-Tkaczyk, K.; Kornitłowicz-Kowalska, T.; Szychowski, K.; Gmiński, J. Biotransformation and toxicity effect of monoanthraquinone dyes during Bjerkandera adusta CCBAS 930 cultures. Ecotoxicol. Environ. Saf. 2020, 191, 110203.
41. Zhang, H.; Zhang, J.; Zhang, X.; Geng, A. Purification and characterization of a novel manganese peroxidase from white-rot fungus Cerrena unicolor BBP6 and its application in dye decolorization and denim bleaching. Process. Biochem. 2018, 66, 222–229.
42. Li, H.; Zhang, R.; Tang, L.; Zhang, J.; Mao, Z. Manganese peroxidase production from cassava residue by Phanerochaete chrysosporium in solid state fermentation and its decolorization of indigo carmine. Chin. J. Chem. Eng. 2015, 23, 227–233.
43. Merino-Restrepo, A.; Mejía, F.; Velásquez-Quintero, C.; Hormaza-Anaguano, A. Evaluation of several white-rot fungi for the decolorization of a binary mixture of anionic dyes and characterization of the residual biomass as potential organic soil amendment. J. Environ. Manag. 2020, 254, 109805.
44. Wang, N.; Chu, Y.; Wu, F.; Zhao, Z.; Xu, X. Decolorization and degradation of Congo red by a newly isolated white rot fungus, Ceriporia lacerata, from decayed mulberry branches. Int. Biodeterior. Biodegrad. 2017, 117, 236–244.
45. Kishor, R.; Purchase, D.; Saratale, G.D.; Ferreira, L.F.R.; Bilal, M.; Iqbal, H.M.; Bharagava, R.N. Environment friendly degradation and detoxification of Congo red dye and textile industry

wastewater by a newly isolated Bacillus cohnni (RKS9). Environ. Technol. Innov. 2021, 22, 101425.

46. Asgher, M.; Yasmeen, Q.; Iqbal, H.M.N. Enhanced decolorization of Solar brilliant red 80 textile dye by an indigenous white rot fungus Schizophyllum commune IBL-06. Saudi J. Biol. Sci. 2013, 20, 347–352.
47. Xing, Q.; Zhang, J.; Zhang, X.; Yang, Y. Induction, Purification and Characterization of a Novel Manganese Peroxidase from Irpex lacteus CD2 and Its Application in the Decolorization of Different Types of Dye. PLoS ONE 2014, 9, e113282.